A COMPARISON OF LINEAR AND NONLINEAR SEISMIC TUNNEL–GROUND INTERACTION ANALYSES

Elefterija Zlatanović *(corresponding author)*
University of Niš,
Faculty of Civil Engineering and Architecture
Aleksandra Medvedeva 14, 18000 Niš, Serbia
E-mail: elefterija2006@yahoo.com

Marina Trajković-Milenković
University of Niš,
Faculty of Civil Engineering and Architecture
Aleksandra Medvedeva 14, 18000 Niš, Serbia
E-mail: trajmarina@gmail.com

Dragan Č. Lukić
University of Novi Sad,
Faculty of Civil Engineering and Architecture
Kozaračka 2a, 24000 Subotica, Serbia
E-mail: drlukic.lukic@gmail.com

Stanko Brčić
University of Belgrade,
Faculty of Civil Engineering
Bulevar kralja Aleksandra 73, 11000 Belgrade, Serbia
E-mail: stanko.brcic@gmail.com

Vlatko Šešov
University of Skopje,
Institute of Earthquake Engineering and Engineering Seismology – IZIIS
Todor Aleksandrov 165, 1000 Skopje, Republic of Macedonia
E-mail: vsesov@gmail.com

Keywords

circular tunnel, linear/nonlinear soil behaviour, beam–spring model, plane-strain conditions, simplified dynamic FE analysis, soil–structure interaction

Abstract

In order to study the effects of a seismically induced tunnel–ground interaction, two-dimensional numerical analyses are performed using the sofware ANSYS. The study employs a coupled beam–spring model subjected to earthquake loading that is simulated under pure shear conditions and determined by a free-field ground-response analysis using the code EERA. The properties of the soil material are considered as both linear and nonlinear. The results obtained by linear dynamic analyses are compared with state-of-practice analytical elastic solutions. A comparison of the results of both linear and nonlinear analyses is also performed, and significant differences, as well as important factors influencing the tunnel–ground interaction for both cases, are evaluated.

1 INTRODUCTION

A reliable evaluation of the seismic response of tunnel structures is crucial in civil and earthquake engineering. As the structural design has shifted to the performance design in recent years, the seismic design, accounting for the soil–structure interaction (SSI) effects, becomes more important. The presence of a tunnel structure considerably modifies the free-field ground motion leading to a different seismic response of the tunnel lining. This phenomenon is related to the combined effects of the *kinematic interaction* and the *dynamic (inertial) interaction*. The kinematic interaction is influenced by the inability of a structure to match the free-field deformation. The dynamic interaction is caused by the existence of a structural mass making the effect of inertial force on the response of the surrounding environment, in which case dynamic forces in the tunnel's structure cause the tunnel to deform the soil, thus producing stress waves that travel away from the structure (radiation damping).

The response of the tunnel, which is confined by the surrounding rock or soil, is basically governed by the ground deformation, and the level of the tunnel deformation will depend on the stiffness of the tunnel relative to the stiffness of the surrounding ground. Therefore, an analysis of the tunnel–ground interaction, concerning both the tunnel and the ground stiffness, is required in order to find an accurate tunnel response.

Besides the ratio of the ground and the lining stiffness, another aspect that sensibly affects the response of the tunnel is the shear-stress transmission at the ground–lining interface. Numerous approaches are frequently based on the assumption that the soil behaves in a linear elastic manner and is perfectly bonded to a structure. However, the contact between the soil and the structure is usually imperfect, since slippage as well as separation

often occur in the interface region. Furthermore, the soil region immediately adjacent to the tunnel structure can experience an extensive strain level, thus causing the coupled soil–tunnel system to behave in a nonlinear manner. The soil–structure interaction effects decrease as the relative displacements between the soil and the structure increase.

In many practical situations, the condition of *partial slip* exists. Nevertheless, solutions are usually derived for the two extreme contact conditions: full-slip and no-slip. *The full-slip condition (smooth contact, sliding contact)* between the lining and the ground assumes equal normal displacements and unequal tangential displacements of the medium and lining at the common interface (i.e., no shear stress transmission and no tangential shear force exist). This assumption is used in order to obtain the extreme values of the bending moments and the shear forces in the tunnel lining, and is only valid for the case of a very soft soil or excitations of high intensity. *The no-slip condition (perfect contact, rigid contact, rough interface)* considers equal displacements of the medium and the lining at the common interface (i.e., the continuity of stresses and displacements, and no relative shear displacements exist), and is being adopted to find the maximum values of the thrust acting in the lining. It is usual practice to consider both of the extreme cases and apply the more critical one. For the case of unequal displacements of the structure and the surrounding ground, or the existence of a locally concentrated mass in the structure, the effect of inertia must not be overlooked. Nowadays, intensive studies are being performed regarding the effect of the interface friction on the tunnel liner's internal forces due to the seismic S- and P-wave propagation [1].

2 THEORETICAL BACKGROUND

The seismic response of circular tunnels has been the focus of a number of studies. Owen and Scholl [2] proposed the response of circular tunnels to an earthquake action to be described by axial compression/extension, longitudinal bending, and ovaling. Considering these deformation modes, it is suggested that the most critical deformation pattern of a circular tunnel is the ovalisation of the cross-section caused by the shear S-waves propagating in the planes perpendicular to the tunnel axis. Therefore, a number of simplified approaches have been developed to quantify the seismically induced ovaling effect on circular tunnels, which is commonly modelled as a two-dimensional, plane-strain condition. The so-called *free-field deformation approach* [3, 4] is based on the theory of wave propagation in an infinite, homogeneous, isotropic, elastic medium, and does not account for any soil–structure interaction effect. In addition, there are analytical solutions after various authors [5-11] that represent the so-called *soil–structure interaction approach*. They are based on the theory of an elastic beam on an elastic foundation, which takes into account the soil–structure interaction (SSI) effects in a quasi-static manner, ignoring any inertial interaction effect. An extensive review of the aforementioned methods can be found in Hashash et al. [12]. A simple modification in order to improve the accuracy of the widely used closed-form elastic solutions considering the kinematic interaction between the tunnel and the ground is suggested by Billota et al. [13]. In addition, expressions for earthquake-induced displacements and the accumulated internal lining forces related to circular tunnels embedded in a rock medium for near-fault conditions are developed by Corigliano et al. [14]. A set of closed-form expressions to calculate the circular tunnel liner's forces due to compressional seismic P-wave propagation is presented in [15]. Both no-slip and full-slip interface conditions were considered and the obtained results were compared and verified against dynamic numerical analyses.

These two approaches include various sub-methods characterised by different levels of approximation depending on the design stage, a knowledge of the geologic setting, and geotechnical parameters. Concerning the types of analyses, they can be grouped into three categories, i.e., *pseudo-static, simplified dynamic*, and *full (detailed) dynamic analysis*, regarding the increasing levels of complexity in the analytical models, soil characterisation, and a description of the seismic input. In pseudo-static methods, the ground–tunnel analysis is uncoupled. The seismic input is reduced to the peak-strain amplitude, computed by simplified formulas based on simple assumptions of harmonic plane S-wave propagation in a homogeneous, isotropic, elastic medium, and then considered to be acting on the tunnel lining in static conditions. In this way the effects of tunnel shape and stiffness on the seismic ground behaviour are ignored. In a simplified dynamic analysis, the soil straining in the range of depths corresponding to the tunnel section, between the tunnel crown and the invert, is computed through a free-field, one-dimensional, site seismic response (SSR) analysis, and then applied to the tunnel lining, again in pseudo-static conditions. In such a way both the acceleration time history and the site characteristics are taken into account, whereas the kinematic soil–structure interaction is still neglected. Moreover, the effects of compressional waves are also neglected, as only the shear waves are considered, which propagate in vertical planes inducing shear strain. In a

full dynamic analysis, the force increments in the lining due to an earthquake are directly obtained as an output of the numerical modelling (such as the dynamic finite element or finite difference methods) adopted for the simulation of the shaking of the coupled ground–tunnel system. In this way, besides the acceleration time history and the site characteristics, both the kinematic and dynamic interactions are also taken into consideration. All the above-presented analyses are reviewed by Billota et al. [16].

The mechanical behaviour of the soils can be relatively complex, even under static conditions, and particularly under seismic impact, in which case the soil is cyclically loaded. Accordingly, there was a need to modify the linear approach in order to provide a reasonable estimation of the ground response to an earthquake action. Experimental results have suggested that some energy is dissipated, even at a very low strain level, thus indicating that the damping ratio of a soil is never zero. It is also suggested that both the soil's shear modulus and the damping ratio are dependent on the shear-strain level. To describe the degradation of the shear modulus and the increase of the damping ratio along with the shear-strain level increase, different curves were proposed in the literature for various types of soils [17]: fine-grained soils, sand, and gravel. The previously mentioned soil models are *equivalent linear models*, and are the simplest and most commonly used. However, they have a limited ability to represent the most significant aspects of soil behaviour under cyclic loading conditions. Equivalent linear models represent only an approximation of the actual nonlinear behaviour of the soil. For that reason they are not proposed to be used directly for problems concerning permanent ground deformation or failure, because they imply that the strain always returns to zero after the cyclic loading. Consequently, since a linear material has no limiting strength, it is not possible to achieve soil failure. And yet, the assumption of linearity allows a very efficient class of constitutive models to be used for ground-response analyses, particularly for problems involving low strain levels such as stiff soil deposits and weak input motions.

Considering the complexity and the high computational cost of dynamic FE analyses, the present study employs simplified dynamic analyses to investigate the seismic response of tunnels that are interacting with the surrounding environment. Although such simplified methods cannot properly simulate the soil stiffness and strength changes that take place during an earthquake and they ignore any dynamic soil–structure interaction effects, they give a reasonable evaluation of the seismic loads regarding an initial estimation of the strains and deformations in a tunnel [18].

A beam–spring model was chosen for the analyses, since, despite its simplicity, it allows relative contributions of partial influences in the total internal lining forces, such as the earthquake-induced displacements, soil shear stress, and tunnel section inertia, to be studied separately.

As noted previously, various analytical studies have suggested that the most critical deformation of a circular tunnel is the ovaling of the cross-section that is caused by shear waves that propagate in planes perpendicular to the tunnel axis, which implies a stress concentration at the tunnel's soffits (shoulder and knee locations of the lining). Therefore, the models were subjected to simple shear conditions obtained by means of a one-dimensional site seismic response (SSR) analysis that neglects the effects of the tunnel's shape and stiffness on the seismic behaviour of a soil. In addition, this analysis ignores the effects of all but vertically propagating shear waves. The free-field soil deformations caused by the wave propagation are calculated for both linear and nonlinear soil behaviour. Thereafter, the calculated soil displacements were applied to beam–spring models in order to simulate earthquake-induced ovalisation under simple shear conditions. Furthermore, the computed deformations are used to calculate the seismic force increments in the tunnel lining by means of closed-form elastic solutions after Wang [9] and Penzien (2000) [11]. The obtained numerical results from the simplified dynamic linear analysis were compared with the analytical solutions. Lastly, significant differences between the linear and nonlinear tunnel–ground interaction analyses were estimated and summarised.

3 GROUND CONDITIONS AND TUNNEL CHARACTERISTICS

The analytical and numerical simulations were performed on a virtual example considering idealised tunnel and ground conditions. The tunnel structure of a circular cross-section is placed within a 30-m-thick soil deposit of medium-dense sand overlying a relatively stiff bedrock, with an overburden cover of 12 m and an axis depth of 15 m. An external tunnel radius of 3.0 m was used, whereas the thickness of the lining is 0.3 m. The physical properties of the tunnel lining and the ground material surrounding the tunnel are reported in Fig. 1.

The shear wave velocity profile $V_s(z)$, illustrated in the given figure as well, was required for a one-dimensional, nonlinear, seismic site reponse analysis completed using the software EERA. The dashed line represents an average value of the shear wave velocity within the soil medium needed for the purpose of the 1D linear SSR analysis.

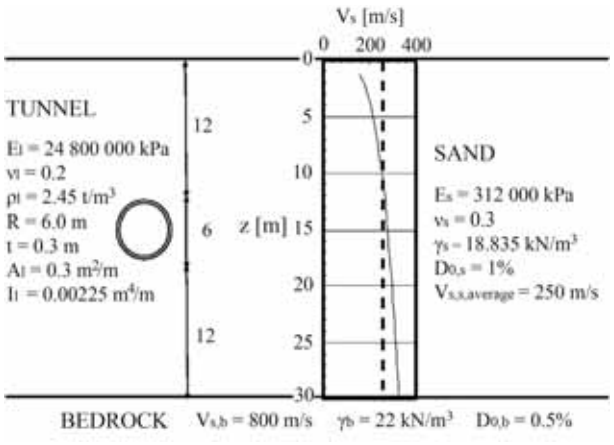

Figure 1. Soil profile and tunnel characteristics (reproduced after Billota et al., 2007 [16]).

4 DESCRIPTION OF THE NUMERICAL MODELS

The present study employs a two-dimensional, coupled beam–spring model using the finite-element-based simulation platform ANSYS [19] to examine the soil–tunnel structure interaction phenomenon. The problem has been analysed and the results of both linear and nonlinear analyses are then compared.

The following assumptions are adopted in the analyses:

1) The soil material surrounding the tunnel is assumed to be a homogeneous and isotropic half-space;
2) The tunnel lining is assumed to behave in a linear elastic manner, whereas the properties of the soil material are considered to be both linear and nonlinear;
3) Two-dimensional, plane-strain analyses were performed, thus assuming the uniform nature of the tunnel's structure and the soil deposit throughout the tunnel's length.

4.1 Discrete coupled beam–spring model (software ANSYS)

The ANSYS 2D discrete model consists of 36 two-noded Timoshenko beam elements (BEAM188) for the tunnel lining and 72 two-noded bi-linear spring elements (COMBIN14) for the soil, placed in the radial (36) and tangential directions (36 elements). At each node there are 3 DOF (*Ux*, *Uy*, *ROTz*) for the beam, and 1 DOF (*Ux*) for the spring elements. The main purpose of the spring elements is the ground–structure interaction modelling, completed by supports placed radially and tangentially (discrete contact). The tied-degrees-of-freedom boundary condition was applied along the interface of the tunnel's lining and the surrounding soil-springs, in order to constrain the nodes of both beam and spring elements to deform identically for the purposes of a no-slip condition simulation, assuming compatible displacements of the lining and the ground [20].

Prior to all the 2D simplified dynamic analyses presented in this study, a static analysis was undertaken in order to check the model for static conditions as well. A static analysis should be performed in order to verify the safety of the tunnel under static conditions, meaning that the tunnel's structure should be stabilised by a balance between the weight of the overburden cover, the reaction force from the ground below, and the lateral soil pressure (Fig. 2(a)).

The emphasis on the inertial effects of surface structures (Force Method) is in stark contrast to the design of underground structures, in which case the seismic design loads are characterised in terms of deformations and strains imposed on the structure by the surrounding ground. Thus, the seismic response of underground structures is controlled by the earthquake-induced ground strain field and its interaction with the structure. This led to the development of design methods such as the Seismic Deformation Method that explicitly considers the seismic deformation of the ground [21].

In the simplified dynamic analysis, on the basis of the seismic deformation method, a beam–spring model illustrated in Fig. 2(b) was used. The interaction between the soil and the tunnel was simulated by a coupled-type interaction spring consisting of a radial and a tangential soil spring. According to the seismic deformation method, seismic forces acting on the beam–spring model were assumed to be the result of the seismically induced ground displacements, the ground shear stress, and the inertial force. The maximum relative displacement between the top and the bottom of the tunnel's cross-section was considered in the analysis.

For the purpose of the given analyses, the properties of soil springs were determined after expressions given by a number of authors: St. John and Zahrah [4], Matsubara and Hoshiya [22], ALA-ASCE [23], and Verruijt [24]. After conducting a series of numerical tests, the value of the soil spring stiffness that was finally adopted in the analyses was according to ALA-ASCE [23] (Table 1). It was the smallest obtained value for the soil spring constants, and the only one for which it was possible to successfully simulate the elastic subgrade reaction in the static analysis. In this way, the flexible surrounding medium was modelled, in which case the soil–tunnel

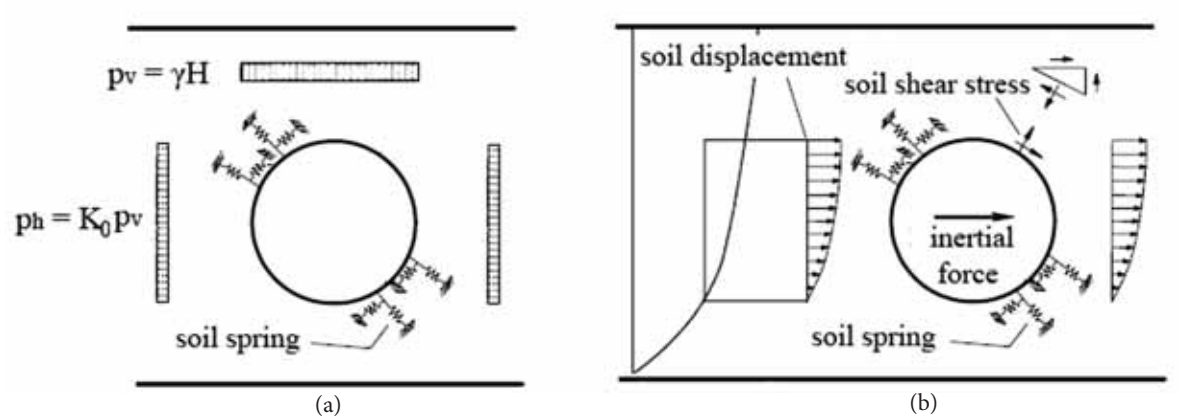

Figure 2. Beam–spring model: (a) static analysis and (b) dynamic analysis. ((b) reproduced after Mizuno and Koizumi, 2006 [21]).

Table 1. Bi-linear spring properties considered in the numerical analyses.

Yield force per unit length of tunnel (kN/m)	Yield displacement (mm)
3085.173	150

interaction is the most pronounced and applying the springs in the model is meaningful. Furthermore, for large frequencies the spring is much more flexible, resulting in smaller values of the spring constant. Therefore, the chosen spring coefficient simulates the soil in a proper way under both static and dynamic conditions.

4.2 One-dimensional SSR analysis (code EERA)

The SSR analyses were carried out using the code EERA [25], which stands for Equivalent-linear Earthquake site Response Analysis. The input of the data and the output of the results are completely integrated with the program MS Excel. This code is intended to perform analyses for linear and equivalent linear stratified subsoils. The code is based on the assumption of vertically propagating, horizontal shear SH-waves through a horizontally layered soil deposit. The horizontal soil layers are represented by a Kelvin–Voigt solid, in which case the soil column is discretised into individual layers using a multi-degree-of-freedom, lumped-parameter model. Shear moduli and viscous damping characterise the properties of the soil layer.

The equivalent linear approach is based on the assumption that both the shear modulus and the damping ratio depend on the shear-strain level, in order to account for some types of soil nonlinearities. For a given input excitation and an initial evaluation of the shear modulus and the damping values, an effective shear strain equal to 65% of the peak strain [17] is computed for a given soil layer. Based on the modulus degradation and the damping curves, revised values of the shear modulus and damping are then obtained. The solution process is developed as a frequency-domain (FD) analysis and an iterative scheme is required to approach a converged solution.

The EERA code allows the bedrock to be modelled as rigid, by choosing the option "inside", or as elastic, by assigning it as the last layer and selecting the option "outcrop". For the purpose of the signal transformation from the outcropping rock to the bedrock, placed at the bottom of the soil layer, the code applies a proper transfer function to the input signal. A computation procedure for determining the bedrock motion from a known free-surface motion is known as deconvolution [17].

The source of the dynamic excitation in this research is the acceleration record of the Hyogoken Nanbu (Kobe) Earthquake in Japan in 1995. The seismic signal of the great Kobe Earthquake has been considered for the reason that this event was the most devastating to underground facilities in recorded history. Strong ground-motion data are generally not available at the depths of concern for tunnel structures, so the development of the required ground motions needs to incorporate attenuation effects (the ground motion decreasing with the depth). The surface acceleration record was applied at the outcropping rock and then transformed to the bedrock, placed at the bottom of the soil layer, by applying a suitable transfer function to the input signal (deconvolution).

Fig. 3 illustrates the acceleration time history that was employed in all the SSR analyses. The peak value of the input-acceleration time history is 0.821g (8.05 m/s^2) occurring approximately 8.5 s after the onset of the excitation.

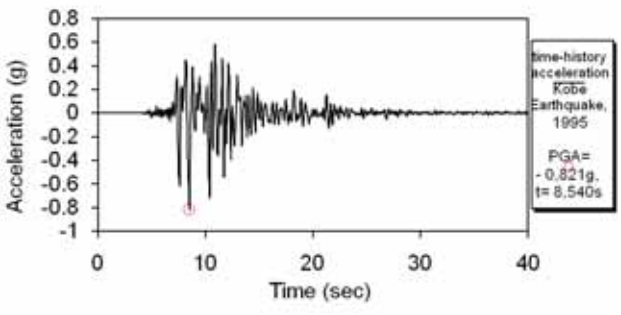

Figure 3. Surface-acceleration record of the 1995 Kobe Earthquake in Japan.

The acceleration, the shear stress, and the strain induced by the seismic waves at the tunnel's depth were calculated using a free-field, one-dimensional SSR analysis. The average soil shear strain, γ_{ave}, as the design free-field shear strain of the soil in the seismic analysis of tunnel structures in the range of depths between the tunnel crown and the invert [26], as well as the corresponding soil shear stress, τ_{ave}, were calculated. The soil straining, i.e., the displacements induced by an earthquake excitation, are then applied through soil springs to the tunnel section of the ANSYS's beam–spring model in a pure shear condition, whereas the soil shear stress was applied directly to the tunnel's lining. In such a way, both the acceleration time history and the site characteristics are taken into account, considering the kinematic tunnel–soil interaction in an approximate way. However, the dynamic soil–structure interaction is ignored.

5 COMPARISON OF THE LINEAR AND EQUIVALENT-LINEAR 1D SSR ANALYSIS RESULTS FOR A SOIL COLUMN

In the present analyses, the ground conditions and the soil behaviour are modelled according to Fig. 1. The free-field soil deformations caused by the wave propagation are calculated for the cases of the linear elastic and nonlinear types of soil behaviour.

In the linear analysis (Fig. 4(a)) it is assumed that the **shear-wave propagation velocity** is constant. For the given soil column, an average value of the shear-wave velocity profile of 250 m/s was used throughout the analysis. In the equivalent-linear analysis, the shear-wave velocities change with the depth of the soil column, as illustrated in Fig. 4(b).

When it comes to a **soil's shear modulus**, in the linear analysis it is assumed to be constant, regarding a constant value of the shear-wave velocity along the soil-

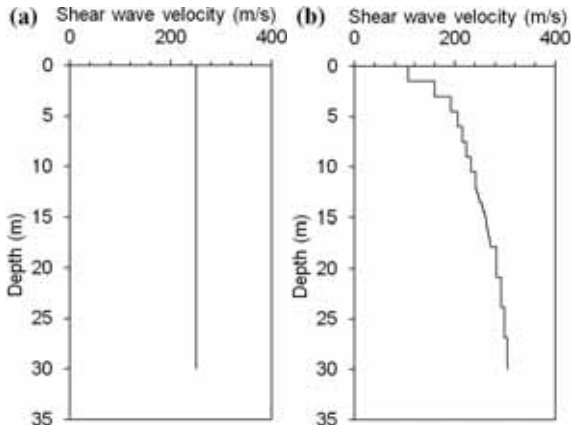

Figure 4. Shear wave velocity profile: (a) linear SSR analysis and (b) equivalent-linear SSR analysis.

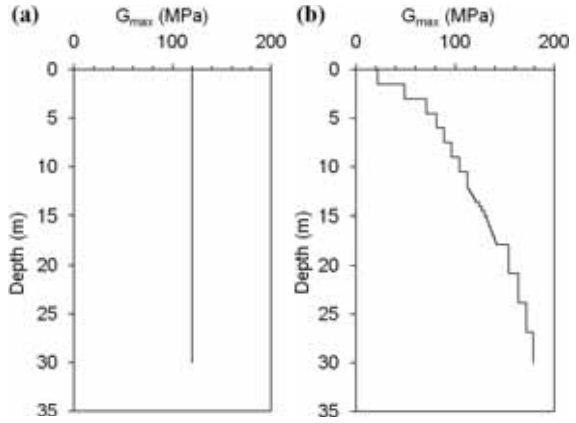

Figure 5. Maximum values of soil shear modulus: (a) linear SSR analysis and (b) equivalent-linear SSR analysis.

column depth (Fig. 5(a)). Its value is G_{max} = 120 MPa. In the equivalent-linear analysis, in accordance with a non-uniform shear-wave velocity profile, the shear modulus is not constant and changes with the depth of the soil column (Fig. 5(b)).

Besides a constant value within the soil column depth, for the case of the linear analysis the soil's shear modulus does not depend on a soil's shear strain level either (G/G_{max} = 1). The value of the **damping ratio** is also constant in the linear approach, and for the sand soil material it is taken to be $D = D_0$ = 1%. In the equivalent linear analyses, for the considered sandy soil material, the equivalent linear soil model as proposed by Seed and Idriss in 1970 (shear-modulus curve) [27] and Idriss in 1990 (damping-ratio curve) [28] was used (Fig. 6). The plot illustrates the prominent properties of the nonlinear soil behaviour – a dependence of both the soil's shear modulus and the damping ratio on the soil's

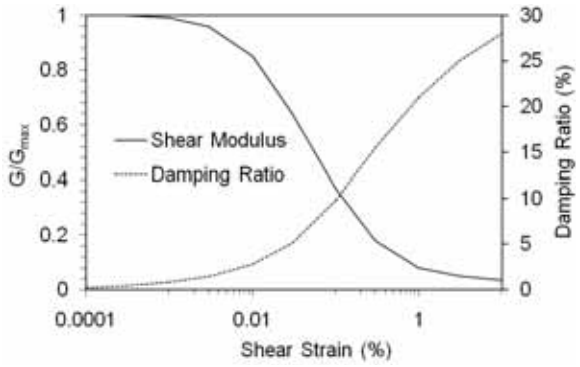

Figure 6. Equivalent-linear model for sand used in EERA code [25].

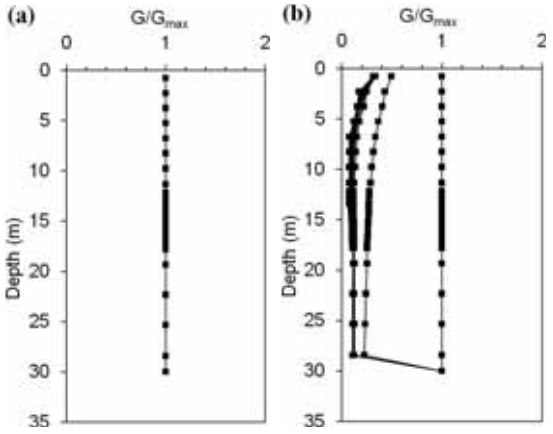

Figure 7. Soil shear modulus ratio G/Gmax: (a) linear SSR analysis and (b) equivalent-linear SSR analysis.

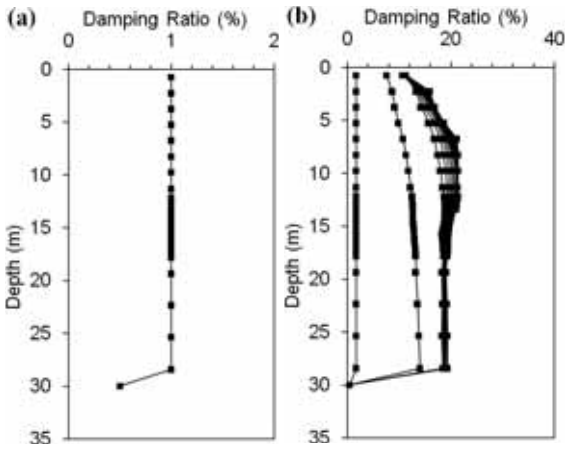

Figure 8. Soil damping ratio: (a) linear SSR analysis and (b) equivalent-linear SSR analysis.

shear-strain rate, i.e., the shear modulus degradation and the damping ratio increase, being influenced by the soil's shear-strain increase. For the previously reported soil properties, diagrams of the soil's shear-modulus ratio

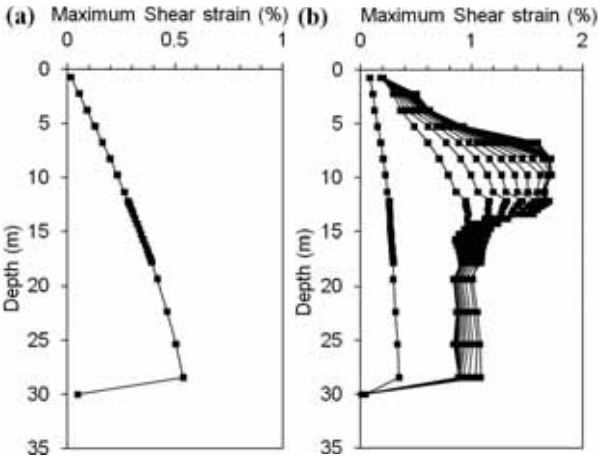

Figure 9. Maximum soil shear strain: (a) linear SSR analysis and (b) equivalent-linear SSR analysis.

G/G_{max} and the damping ratio throughout the soil column are illustrated for the cases of linear and equivalent-linear analyses in the following plots (Fig. 7(a)–(b) and Fig. 8(a)–(b)).

The linear EERA analysis showed that for the given soil profile and input excitation, the **maximum soil shear strain** is 0.54%, and its average value at the tunnel's location (at depths between the crown and invert) is 0.34% (Fig. 9(a)). In the equivalent-linear analysis, the maximum soil shear deformation is 1.72%, whereas its average value at the tunnel's location is 1.16% (Fig. 9(b)). Accordingly, the linear analysis underestimates the soil's shear strain significantly, because with the assumed constant damping ratio of the soil, it neglects the fact that along with a shear-strain level increase (i.e., soil weakening), a soil damping ratio, as well as the possibility of the soil absorbing a portion of the seismic energy, are being increased too, which, on the other hand, is predicted by the equivalent-linear analysis. The seismic energy absorption of the soil (hysteretic energy dissipation) at the level of the tunnel's centre-line for both analyses is illustrated in two subsequent plots (Fig. 10(a)–(b)).

Regarding the **soil's shear stress**, its maximum value obtained from the linear analysis is 646.69 kPa, and the average value at the tunnel's location between 12 and 18 m of the given soil profile is 406.25 kPa. In the equivalent linear analysis, the calculated maximum soil shear stress is 199.45 kPa, whereas its average value between the top and the bottom of the tunnel section is 150.99 kPa. In conclusion, the linear analysis overestimates the soil's shear stress values, since, unlike the equivalent linear soil model, it does not take into account the shear-modulus reduction with the soil's shear-strain amplitudes due to the constant soil shear modulus assumption (Fig. 11(a)–(b)).

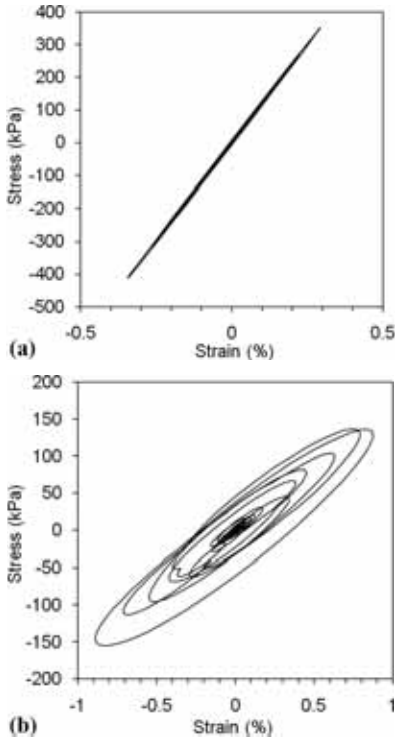

Figure 10. Soil hysteretic energy dissipation at the tunnel's centre-line location: (a) linear SSR analysis and (b) equivalent-linear SSR analysis.

The **peak ground acceleration** at the ground surface is another aspect included in the EERA code SSR analysis (Fig. 12(a)–(b)). For the case of the linear analysis, the maximum ground acceleration value is 1.57g, and at the level of the tunnel's axis it is equal to 1.30g. In the equivalent linear analysis, a_{max} = 1.04g, and at the tunnel spring-line location, it is 0.61g. Hence, the linear analysis gives higher peak ground-acceleration values due to the assumption of a constant damping ratio for the soil. In the equivalent linear analysis, however, the ground-acceleration values are significantly lower. This is correlated with the nonlinear soil property corresponding to the increasing percentage of damping along with the soil's shear-strain increase (i.e., soil weakening), and by that, the soil's ability to absorb a part of the seismic wave energy, which finally results in considerably lower values for the ground acceleration.

The effects of soil damping are illustrated in the figures related to the **amplification ratio** of the ground acceleration at the surface to the acceleration at the bedrock underlying the 30-m-thick soil layer. The linear analysis resulted in an amplification ratio of up to 3.5 and, as can be seen from Fig. 13(a), the amplification function has a number of peaks corresponding to the natural frequencies of the layer, indicating an amplitude decrease with higher frequencies in a slower manner due to the constant

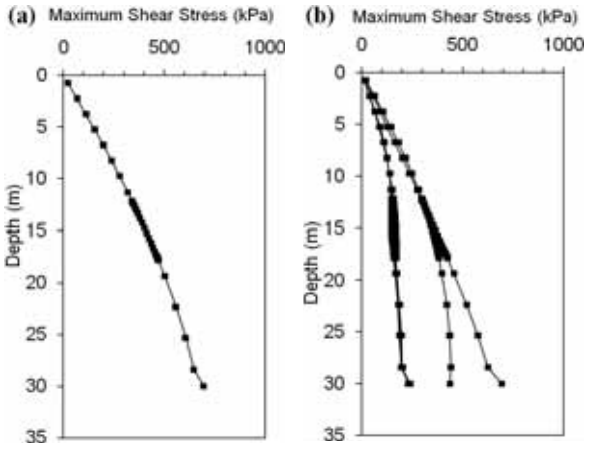

Figure 11. Maximum soil shear stress: (a) linear SSR analysis and (b) equivalent-linear SSR analysis.

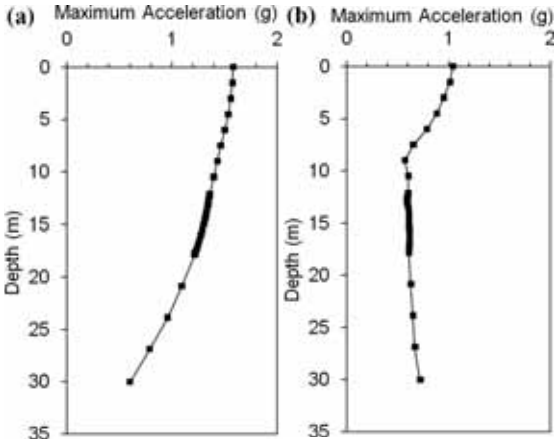

Figure 12. Peak ground acceleration: (a) linear SSR analysis and (b) equivalent-linear SSR analysis.

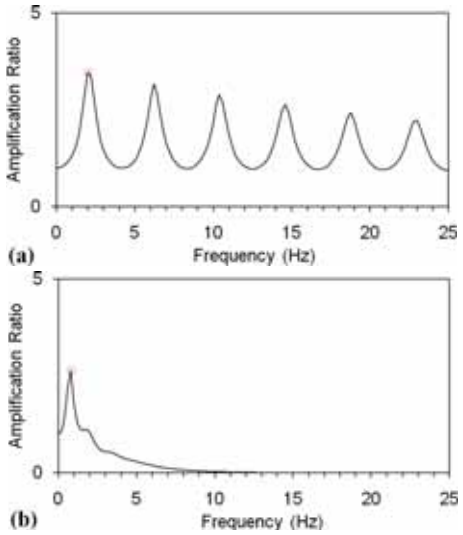

Figure 13. Amplification ratio: (a) linear SSR analysis and (b) equivalent-linear SSR analysis.

soil damping ratio. On the other hand, the amplification function computed by the equivalent-linear analysis resulted in a somewhat lower maximum (2.6), with only a couple of peaks (Fig. 13(b)), due to the prominent soil nonlinearities and high damping values related to the relatively rapid absorption of the seismic wave energy.

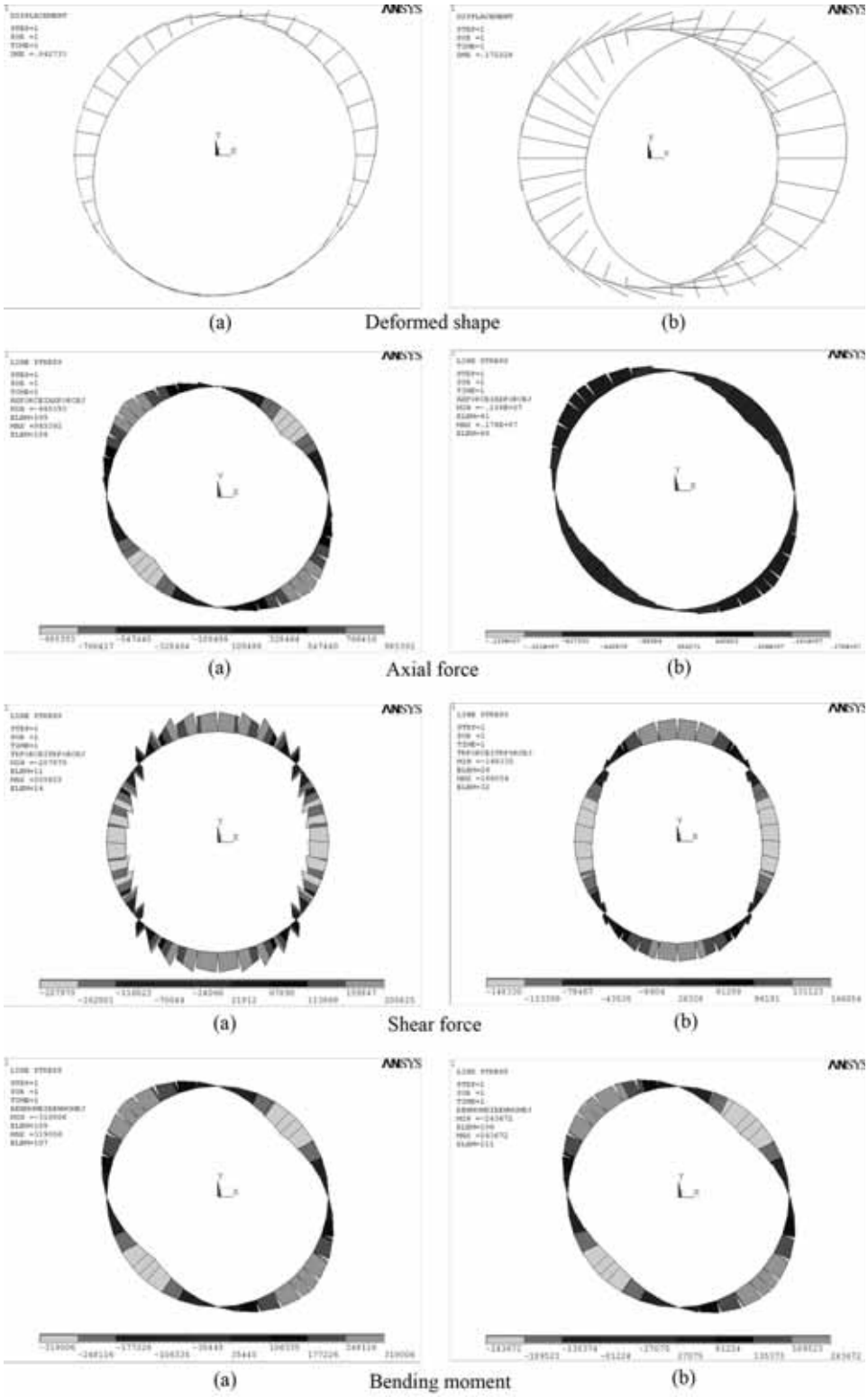

Figure 14. Ovalisation and lining force distributions: (a) linear and (b) nonlinear SSI analysis.

6 ANSYS OUTPUT PLOTS OF LINEAR AND NONLINEAR SOIL–TUNNEL INTERACTION ANALYSES

The corresponding beam–spring numerical model of the linear and nonlinear soil–tunnel interaction analysis was made using ANSYS. The output plots are given for the case of the total loading: earthquake, tunnel section inertia, and soil shear stress. Referring to an ovalisation of a transverse section of the tunnel's lining, all the ANSYS output plots (Fig. 14(a)–(b)) confirmed that the beam–spring model has simulated this deformation pattern successfully in both the linear and nonlinear SSI analyses, since the maxima of the thrust and the bending moment occur at the shoulder and knee locations (θ = 45°, 135°, 225°, and 315°), whereas the extreme values of the transversal force occur at the tunnel crown, abutments, and invert locations of the lining (θ = 0° (360°), 90°, 180°, and 270°).

7. COMPARISON OF LINEAR AND NONLINEAR SOIL–TUNNEL STRUCTURE-INTERACTION ANALYSES

7.1 Comparison of the numerical linear analysis and analytical solutions

First, the results of the simplified dynamic linear analyses are compared to the closed-form elastic solutions related to earthquake-induced sectional forces in the tunnel lining (Fig. 15). The internal forces in the lining are functions of the free-field shear strain γ_{ave} [29]. The considered strain is the average value between the depths corresponding to the crown and the invert of the tunnel. In this work, the state-of-practice analytical expressions by Wang, 1993 [9] and Penzien, 2000 [11] were used, which refer to the tunnel and ground properties corresponding to Fig. 1. In the analyses described here, only the case of a no-slip condition was considered, since it results in maximum values of thrust. Under the assumption of a rough interface between the lining and the soil (assuming compatible displacements of the lining and the ground), the variation of thrust (N), shear force (T), and bending moment (M) in terms of the angle θ is calculated according to equations given by the aforementioned authors. The angle θ is measured counter clockwise with respect to the x-axis.

In applications of the beam–spring model, conducting a simplified dynamic analysis in a simple shear condition, it is quite usual to take into account only the earthquake-induced displacements and eventually the tunnel section's inertial force, without considering the influence of the soil's shear stress. In relation to that, two cases have been analysed in the present study: a beam–spring model without considering the seismically induced soil shear stress and a beam–spring model that involves the soil's shear stress, in order to estimate the error when the shear stress of the soil medium is not accounted for. The common conclusion that can be drawn regarding all the forces in the tunnel's lining is that excluding the soil's shear stress from the coupled beam–spring model, in order to simulate SSI effects, yields a considerable underestimation of the internal lining forces.

With regard to the **thrust** distribution around the lining, considering Wang's solution [9], the beam–spring model, when accounting for the soil's shear stress, provides a fairly consistent distribution of the N-force. On the other hand, the beam–spring model without the soil's shear stress consideration greatly underestimates the values of the axial force, approximately the same as Penzien's solution [11], thus confirming the conclusions of the study by Hashash et al. [30] that Penzien's approach predicts much lower thrust values than those predicted by Wang's method.

Accordingly, ignoring the soil's shear stress in a simplified dynamic analysis by using a beam–spring model yields an error that cannot be tolerated, since the contact between the structure and the surrounding ground in the model is defined in a discrete manner, only at a number of points. On the other hand, such a beam–spring model results in the thrust distribution being approximately the same as obtained with Penzien's approach. This implies that Penzien's methodology severely underestimates the seismically induced maximum thrust in the tunnel's lining under the no-slip assumption for the reason of a lack of implementation of the circumferential stiffness of the tunnel–ground system (resistance to compression), which is in accordance with the remarks in [29], and, because of that, it should be avoided.

Referring to all of the previously mentioned, it can be concluded that, in order to develop reliable simulations and obtain relevant results, a beam–spring model in a simplified dynamic analysis should take into consideration, besides the earthquake-induced soil displacements and the tunnel's inertial force, also the soil's shear stresses.

Furthermore, the distributions of the **transverse forces** and the **bending moments** along the tunnel's lining according to the analytical and numerical results are also illustrated in the same plots (Fig. 15). It should be pointed out that in Wang's approach an expression for the transverse forces does not exist. The presented distribution of the shear forces is opposite to that of Penzien's

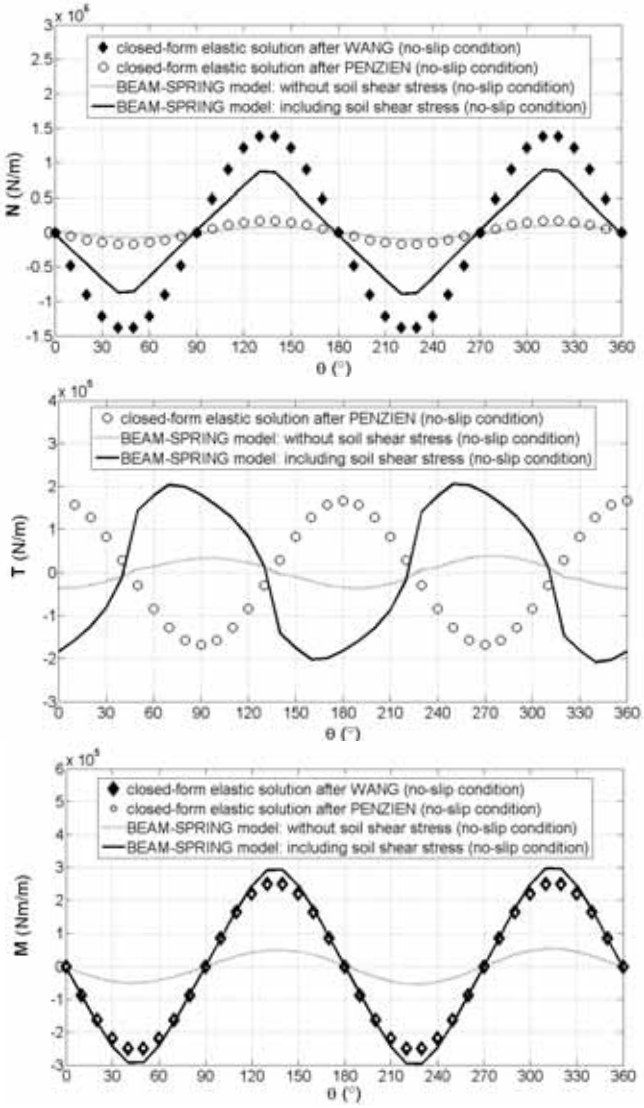

Figure 15. Comparison of the linear SSI analysis results with the closed-form elastic solutions.

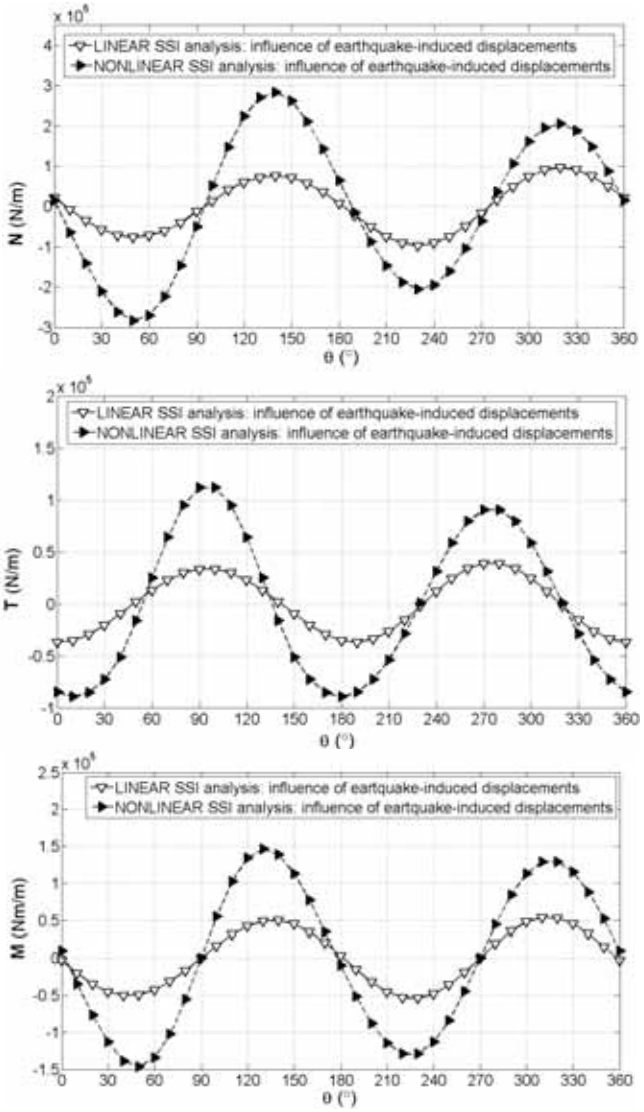

Figure 16. Comparison of thrust, shear force, and bending moment distributions in the tunnel lining computed by the linear and nonlinear SSI analyses: influence of earthquake-induced displacements.

solution, since in the ANSYS software the opposite sign convection for T-forces is established. As to the seismically induced shear forces and bending moments, the coupled beam–spring models involving soil shear stress for the no-slip assumption predict the distribution pattern that matches relatively well with the solutions according to Penzien's and Wang's approaches. This is opposite to the discrete models that do not account for the soil's shear stress, in which case the shear-force and bending-moment values are significantly underestimated when compared to the elastic closed-form solutions. Unlike the thrust distribution, the solutions of Wang and Penzien provide consistent distributions of the bending moments (the symbols related to Wang's and Penzien's solutions for *M* practically coincide).

Finally, it can be observed that the magnitude of the thrust has a much greater influence than the moments on the stresses experienced by the tunnel's lining, which is typical for a rough tunnel–ground interface assumption.

7.2 Influence of seismically induced displacements upon the internal lining forces

Based on a comparison of the results of numerical linear and nonlinear analyses regarding the distributions of thrust, shear force, and bending moment in the tunnel's lining due to earthquake-induced displacements (Fig. 16), the following conclusions can be drawn: the linear analysis, which predicts lower soil shear-strain values, results in smaller soil displacements induced by seismic

shear-wave propagation throughout the sandy soil medium. The maximum displacement values of the tunnel's section are 3.55 cm at the crown and 1.63 cm at the invert locations. Hence, the relative displacement between the top and the bottom of the circular tunnel profile has a lower value (1.92 cm), resulting in a smaller deformation (ovalisation) of the tunnel's cross-section. On the other hand, in the nonlinear analysis, due to a significantly larger soil shearing, the soil displacements are also larger: 17.68 cm at the crown and 12.43 cm at the invert regions. This, of course, results in a greater displacement difference between the top and the bottom of the tunnel's cross-section (5.25 cm) when compared to the linear analysis, which also leads to significantly greater ovalisation of the tunnel's structure.

In conclusion, a linear analysis underestimates the soil's shear strain and, consequently, underestimates the soil displacements due to earthquake action, thus leading to a significant underestimation of the internal lining forces.

7.3 Influence of the soil's shear stress upon the internal lining forces

From the seismically induced soil shear-stress viewpoint, according to Fig. 17, the results are the following: in the linear analysis, the soil shear modulus is constant and does not depend on the soil shear deformation, thus resulting in higher values for the soil's shear stress. In contrast to that, the nonlinear analysis gives significantly lower values for the soil's shear stress, since

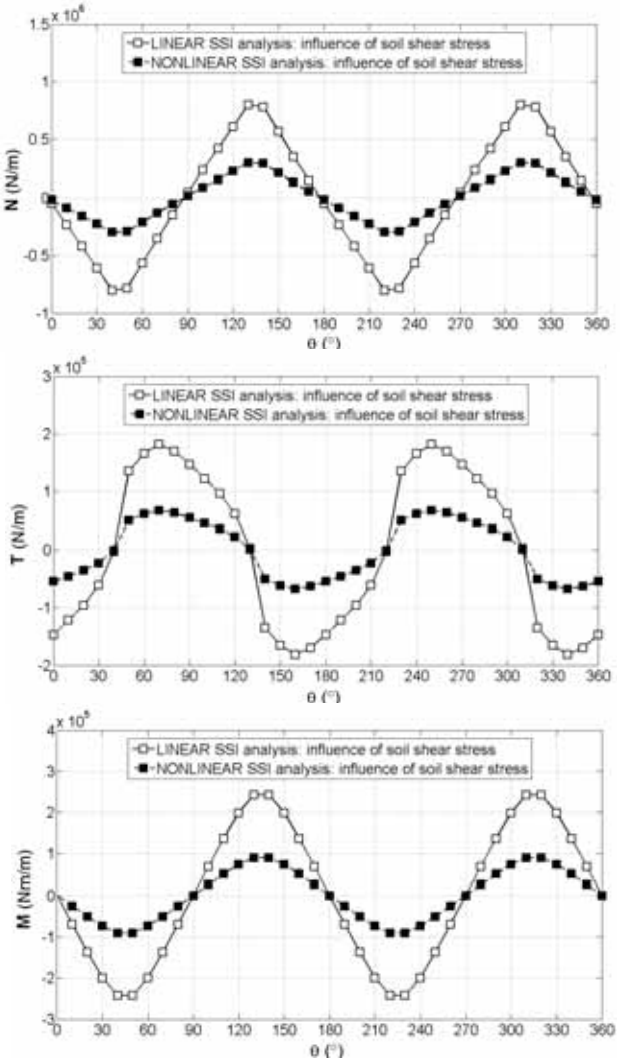

Figure 17. Comparison of thrust, shear force, and bending moment distributions in the tunnel lining computed by the linear and nonlinear SSI analyses: influence of soil shear stress.

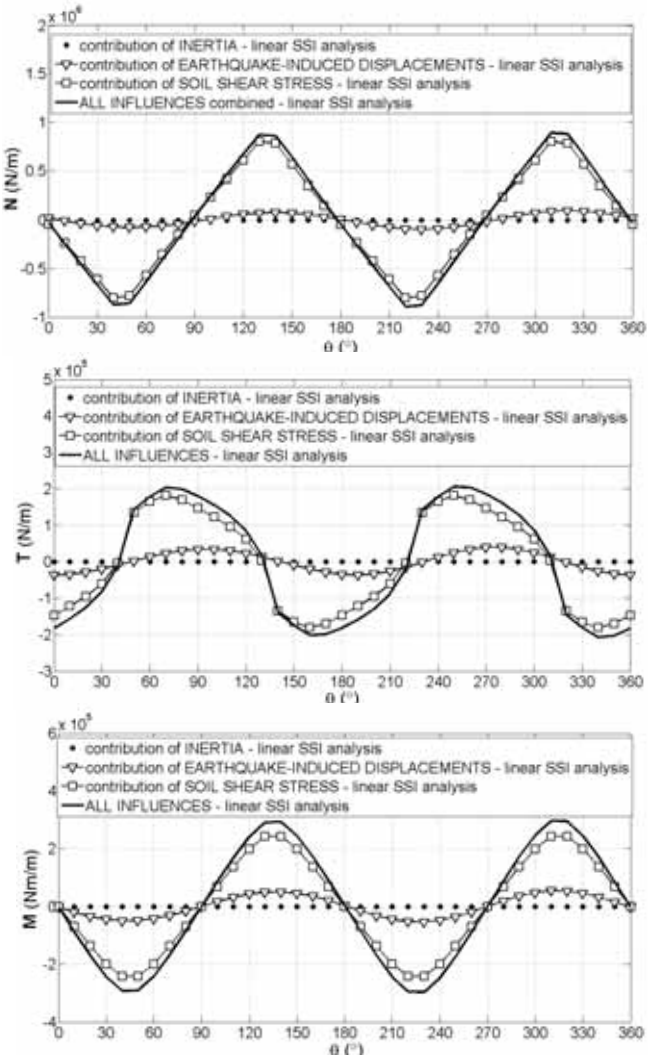

Figure 18. Contribution of earthquake-induced displacements, tunnel section inertial force, and soil shear stress to thrust, shear force, and bending moment distributions in the tunnel lining computed by the linear SSI analysis.

the nonlinear soil model accounts for the soil's shear-modulus degradation with the increase of the soil's shear strain. Hence, it can be observed that a linear analysis represents a conservative solution because it predicts unrealistically high values for the soil's shear stress.

7.4 Influence of the tunnel section inertia upon the internal lining forces

Regarding the inertial force of a tunnel section, it has a higher value in the linear analysis, considering the significantly higher computed values of the ground acceleration in comparison with the nonlinear analysis, as a consequence of the assumption of a constant damping ratio, typical for the linear soil behaviour. In the case of soil behaving in a nonlinear manner, the value of the tunnel section inertial force is considerably lower, owing to the lower ground acceleration, due to the soil's ability to absorb a seismic energy to some extent, and therefore, to enlarge the shearing deformations, resulting in stronger damping abilities. Therefore, a linear analysis overestimates the inertial forces.

7.5 Relative contributions of the partial influences in the total internal lining forces

Referring to the formerly discussed tunnel section inertia, on the basis of the plots given in Fig. 18 and Fig. 19, it can be seen that the relative contribution of the inertial force in the total of the internal lining forces is

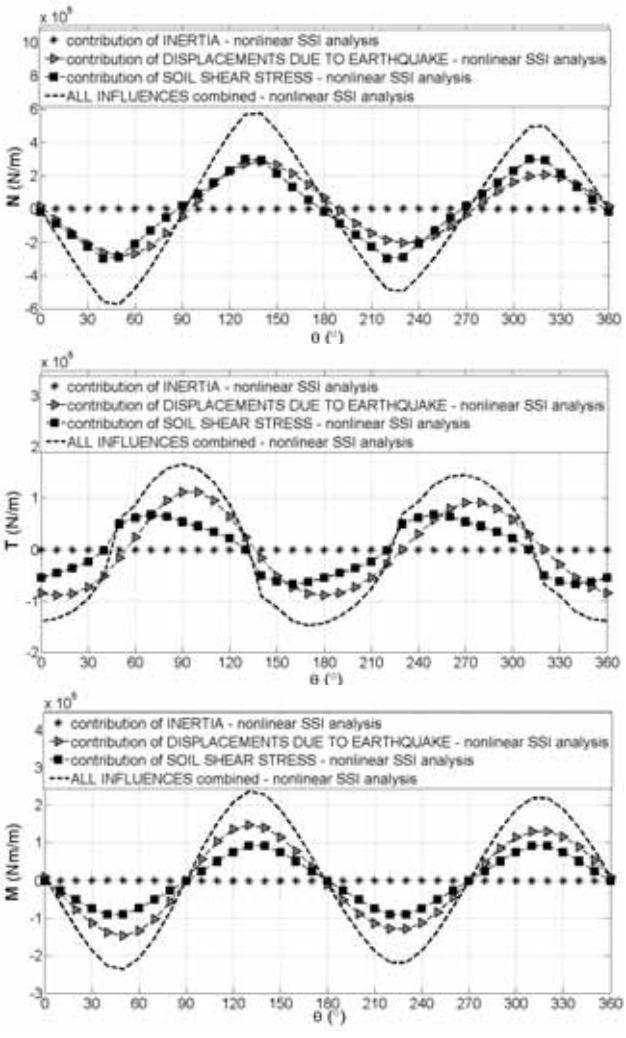

Figure 19. Contribution of earthquake-induced displacements, tunnel section inertial force, and soil shear stress to thrust, shear force, and bending moment distributions in the tunnel lining computed by the nonlinear SSI analysis.

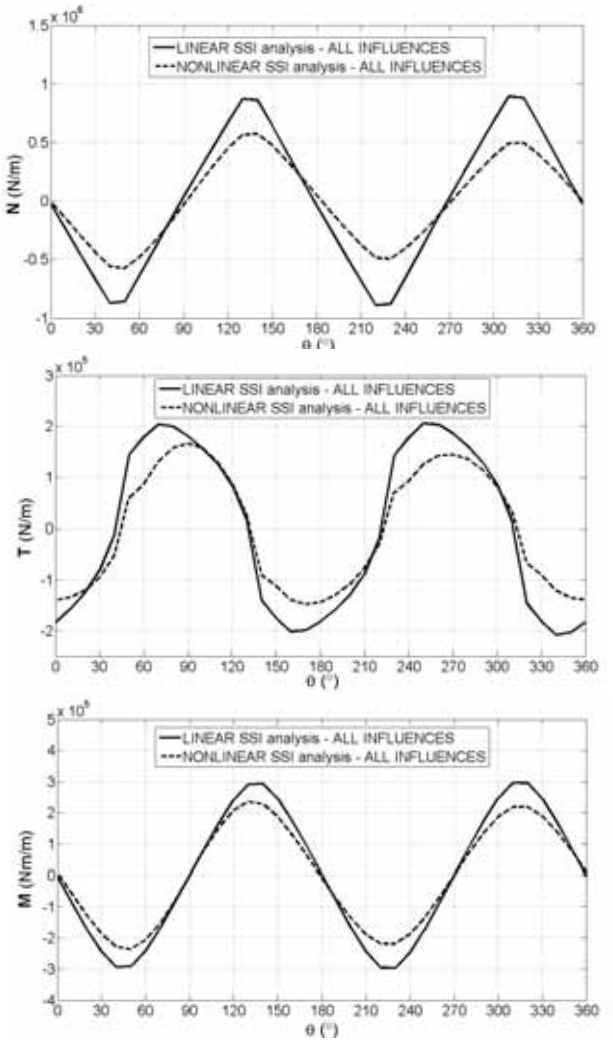

Figure 20. Comparison of thrust, shear force, and bending moment distributions in the tunnel lining computed by the linear and nonlinear SSI analyses: all influences combined (earthquake-induced displacements + tunnel section inertial force + soil shear stress).

negligibly low for the cases of both linear and nonlinear analyses, because it participates in the total lining thrust, shear force, and bending moment distributions by much less than 1%. Considering the relative contributions of the other two factors (i.e., seismically induced displacements and a soil shear stress), there is a quite evident difference between the two types of analysis. According to the results of the linear analysis (Fig. 18), the influence of the soil shear stress is the most dominant in the total distributions of the *N*, *T*, and *M* forces in the tunnel lining. Regarding the results of the nonlinear analysis (Fig. 19), however, earthquake-induced displacements have a predominant influence upon all of the sectional forces, although the contribution of the soil shear stresses is also quite pronounced, particularly in the case of the accumulated thrust.

7.6 Comparison of linear and nonlinear SSI analyses

Taking into consideration the combined effects of all of the influences (i.e., earthquake-induced displacements + tunnel section inertia + soil shear stresses) upon the total distributions of the thrust, shear force, and bending moment in the tunnel lining (Fig. 20), a linear analysis could be considered as the more conservative one for estimating the seismically induced internal lining forces. This is particularly pronounced, as the earthquake excitation and the degree of soil nonlinearities increase.

Although the linear analysis is computationally convenient and provides reasonable results for many practical problems, it presents an approximation of the actual soil–tunnel system response. On the other hand, the nonlinear analysis allows a significant accuracy in simulating the tunnel–ground interaction under earthquake loading conditions due to the fact that the soil behaviour is taken into consideration more realistically regarding its nonlinearity. Nevertheless, more parameters than used for the linear analysis are usually required, the evaluation of which might be complex due to the variability in the soil conditions, the uncertainty in the soil properties, and the scatter in the experimental data upon which many of the input parameters are based. In addition, this analysis suffers from the important disadvantage that the solution time, the computational cost, and the complexity of the analysis are substantially increased.

8. CONCLUDING REMARKS

Considering the analyses described in this paper, related to the simplified dynamic linear and nonlinear analyses of soil–tunnel structure interaction studied by a numerical coupled beam–spring model under no-slip condition, with a special emphasis on the relative contributions of partial influences, such as the earthquake-induced displacements, soil shear stress, and tunnel section inertia, in the total internal lining forces, the following conclusions can be drawn:

– When using the beam–spring model, in order to simulate the SSI effects correctly, soil shear stresses should be taken into account along with seismically induced displacements. It was found that the relative part of the cross-sectional forces induced by the tunnel section inertia is significantly less than 1% of the total computed values for both the linear and nonlinear analyses. This is not surprising, since the tunnel section inertia is negligible relative to the inertia of the surrounding ground. Therefore, the inertial force could be ignored in a numerical model.

– A significant discrepancy in the computed seismically induced lining thrust between Wang's and Penzien's analytical approach is validated. The comparisons with numerical results clearly demonstrate that Wang's solution provides a realistic estimation of the thrust in the tunnel linings for the no-slip condition. Accordingly, Penzien's expression for the seismically induced axial force in the lining under the rough interface assumption should be avoided.

– Linear analysis underestimates the soil shear strain, and consequently also underestimates the soil displacements induced by seismic shear-wave propagation, producing a significant underestimation of the tunnel lining's cross-sectional forces. In addition, it predicts unrealistically higher values of the soil shear stress due to the assumption of a constant soil shear modulus throughout the analysis, thus resulting in higher internal lining forces. From a tunnel inertial force point of view, it overestimates the lining's cross-sectional forces, considering significantly higher computed ground accelerations compared to nonlinear analysis, as a consequence of the constant damping ratio assumption typical for the linear soil behaviour. The influence of the soil shear stress is the most dominant in total distributions of *N, T*, and *M* forces in the tunnel lining.

– Nonlinear analysis, due to a prediction of a significantly larger soil shearing (soil displacements), results in a higher relative displacement between the top and the bottom of the circular tunnel cross-section compared to the linear analysis. This leads to significantly greater ovalisation of the tunnel structure, and therefore to higher values of the internal

lining forces. Unlike the linear approach, a nonlinear analysis gives lower values of the soil shear stress, since the nonlinear soil model accounts for the soil shear modulus reduction, as the soil shear strain increases. In the case of soil behaving in a nonlinear manner, the tunnel section inertial forces are lower owing to lower ground accelerations, due to an increase of the damping ratio with the soil shear strain increase, as well as the nonlinear soil property to absorb a significant portion of the seismic wave energy along with the soil weakening. Earthquake--induced displacements have a predominant influence upon all of the cross-sectional forces, although the relative contribution of the soil shear stresses is also quite significant.

– It seems that the linear analysis can result in a more conservative estimation of the internal forces in the tunnel lining, as the peak acceleration and the level of soil nonlinearity increase.

In order to improve the models and to validate the above drawn conclusions, analyses with more complex models should be performed, in accordance with the most recent achievements in the area of tunnel structures under seismic impact. The interface region between the tunnel lining and the surrounding ground could be more properly simulated as a full-slip contact, with separation allowed under tensile stresses. In addition, the effects of the secondary compressional P-waves, resulting from the shear S-waves scattered by the ground surface, should also be taken into account. Therefore, a possible course of further researches should be in accordance with the former stated remarks, and is an ongoing research activity of the authors of this paper.

Acknowledgement

The authors gratefully acknowledge the support of the Ministry of Education, Science and Technological Development of the Republic of Serbia in the scope of the scientific-research projects TR36028 (2011–2014) and TR36043 (2011–2014).

REFERENCES

[1] Kouretzis, G.P., Sloan, S.W., Carter, J.P. 2013. Effect of interface friction on tunnel liner internal forces due to seismic S- and P-wave propagation. Soil Dynamics and Earthquake Engineering 46, 41-51. doi: 10.1016/j.soildyn.2012.12.010

[2] Owen, G.N., Scholl, R.E. 1981. Earthquake engineering of large underground structures. Report FHWA/RD-80/195, Federal Highway Administration and National Science Foundation, McLean, Virginia.

[3] Newmark, N.M. 1968. Problems in wave propagation in soil and rock. Proc. Int. symp. on Wave Propagation and Dynamic Properties of Earth Materials, Albuquerque, New Mexico, pp. 7-26.

[4] St. John, C.M., Zahrah, T.F. 1987. Aseismic design of underground structures. Tunnelling and Underground Space Technology 2(2), 165-197.

[5] Burns, J.Q., Richard, R.M. 1964. Attenuation of stresses for buried cylinders. Proc. Symp. on Soil–Structure Interaction, University of Arizona at Tempe, Arizona, pp. 378-392.

[6] Hoeg, K. 1968. Stresses against underground structural cylinders. Journal of the Soil Mechanics and Foundations Division, ASCE 94(4), 833-858.

[7] Peck, R.B., Hendron, A.J., Mohraz, B. 1972. State of the art in soft ground tunneling. Proc. Conf. on Rapid Excavation and Tunneling, American Institute of Mining, Metallurgical and Petroleum Engineers, New York, pp. 259-286.

[8] Schwartz, C.W., Einstein, H.H. 1980. Improved design of tunnel supports: Vol. 1 – Simplified analysis for ground–structure interaction in tunneling. Report UMTA-MA-06-0100-80-4, US Department of Transportation, Urban Mass Transportation Administration, Washington DC.

[9] Wang, J.N. 1993. Seismic design of tunnels: a state-of-the-art approach. Parsons, Brinckerhoff, Quade and Douglas, Inc., New York.

[10] Penzien, J., Wu, C. 1998. Stresses in linings of bored tunnels. International Journal of Earthquake Engineering and Structural Dynamics 27(3), 283-300. DOI: 10.1002/(SICI)1096-9845(199803)27:3<283::AID-EQE732>3.0.CO;2-T

[11] Penzien, J. 2000. Seismically induced racking of tunnel linings. International Journal of Earthquake Engineering and Structural Dynamics 29(5), 683-691. DOI: 10.1002/(SICI)1096-9845(200005)29:5<683::AID-EQE932>3.0.CO;2-1

[12] Hashash, Y.M.A., Hook, J.J., Schmidt, B., Yao, J.I.-C. 2001. Seismic design and analysis of underground structures. Tunnelling and Underground Space Technology 16, 247-293.

[13] Billota, E., Lanzano, G., Russo, G., Santucci de Magistris, F., Silvestri, F. 2008. An early-stage design procedure for circular tunnel lining under seismic actions. Proc. 14th World conf. on Earthquake Engineering, Beijing, Paper No. 08-02-0049.

[14] Corigliano, M., Scandella, L., Lai, C.G., Paolucci, R. 2011. Seismic analysis of deep tunnels in near fault

conditions: a case study in Southern Italy. Bulletin of Earthquake Engineering 9(4), 975-995. doi: 10.1007/s10518-011-9249-3

[15] Kouretzis, G.P., Andrianopoulos, K.I., Sloan, S.W., Carter, J.P. 2014. Analysis of circular tunnels due to seismic P-wave propagation, with emphasis on unreinforced concrete liners. Computers and Geotechnics 55, 187-194. http://dx.doi.org/10.1016/j.compgeo.2013.08.012

[16] Billota, E., Lanzano, G., Russo, G., Santucci de Magistris, F., Aiello, V., Conte, E., Silvestri, F., Valentino, M. 2007. Pseudostatic and dynamic analyses of tunnels in transversal and longitudinal directions. Proc. 4th Int. conf. on Earthquake Geotechnical Engineering, Thessaloniki, Paper No. 1550.

[17] Kramer, S.L. 1996. Geotechnical earthquake engineering. Prentice Hall, New Jersey.

[18] Kontoe, S., Zdravkovic, L., Potts, D.M., Menkiti, C.O. 2008. Case study on seismic tunnel response. Canadian Geotechnical Journal 45, 1743-1764.

[19] ANSYS Inc. 2012. ANSYS Documentation, ANSYS Multiphysics. Canonsburg, Pennsylvania. www.ansys.com.

[20] Zlatanović, E., Broćeta, G., Popović-Miletić, N. 2013. Numerical modelling in seismic analysis of tunnels regarding soil–structure interaction. Facta Universitatis, Series: Architecture and Civil Engineering 11(3), 251-267. doi:10.2298/FUACE1303251Z

[21] Mizuno, K., Koizumi, A. 2006. Dynamic behavior of shield tunnels in the transverse direction considering the effects of secondary lining. Proc. 1st European conf. on Earthquake Engineering and Seismology, Geneva, Paper No. 1359.

[22] Matsubara, K., Hoshiya, M. 2000. Soil spring constants of buried pipelines for seismic design. Journal of Engineering Mechanics 126(1), 76-83.

[23] ALA-ASCE. 2001. Guidelines for the design of buried steel pipe. Reston, Virginia. http://www.americanlifelinesalliance.com/pdf/Update061305.pdf.

[24] Verruijt, A. 2005. Soil dynamics. Delft University of Technology, Delft.

[25] Bardet, J.P., Ichii, K., Lin, C.H. 2000. EERA – A computer program for Equivalent-linear Earthquake site Response Analyses of layered soil deposits. University of Southern California, Los Angeles.

[26] Zlatanović, E., Lukić, D., Šešov, V. 2014. Pseudostatic and simplified dynamic methods of design soil shear strain evaluation in seismic analysis of tunnel structures. Izgradnja 68(1-2), 9-19 (in serbian).

[27] Seed, H.B., Idriss, I.M. 1970. Soil moduli and damping factors for dynamic response analyses. Report EERC 70-10, Earthquake Engineering Research Center, University of California, Berkeley.

[28] Idriss, I.M. 1990. Response of soft soil sites during earthquakes. Proc. H. Bolton Seed Memorial Symposium, J.M. Duncan (ed.), Vol. 2, BiTech Publishers, Vancouver, British Columbia, Canada, pp. 273-289.

[29] Zlatanović, E., Lukić, D., Šešov, V. 2014. Presentation of analytical solutions for seismically induced tunnel lining forces accounting for soil–structure interaction effects. Building Materials and Structures 57(1), 3-28.

[30] Hashash, Y.M.A., Park, D., Yao, J.I.-C. 2005. Ovaling deformations of circular tunnels under seismic loading: an update on seismic design and analysis of underground structures. Tunnelling and Underground Space Technology 20, 435-441. doi: 10.1016/j.tust.2005.02.004